Proceedings of 2022 IEEE
International Conference on Mechatronics and Automation
August 7 - 10, Guilin, China

MYO Armband-based a Master-Slave Heterolateral Elbow Joint Rehabilitation Robot System

Hanze Wang, Shuxiang Guo, He Li, Dongdong Bu*

Key Laboratory of Convergence Biomedical Engineering System and Healthcare Technology,The Ministry of Industry and Information Technology, School of Life Science,
Beijing Institute of Technology,

*Corresponding author: guoshuxiang@bit.edu

***Abstract* - Recent years, due to the outbreak of the COVID-19, non-contact rehabilitation medical methods gain traction. The master-slave rehabilitation robot system which meet the good isolation effect has become the equipment that rehabilitation hospitals crave. During treatment, long-term ipsilateral rehabilitation guidance will easily cause muscle fatigue in the physiotherapist's guiding arm, while part of heterolateral control (like foot-hand control) may reduces the rehabilitation effect. In order to balance that, in this paper, a novel master-slave heterolateral elbow joint robot rehabilitation system is proposed. Physiotherapist control the patient's heterolateral elbow joint robotic arm through the MYO armband, enabling the physiotherapist to observe the patient's movements more intuitively while maintaining a safe distance from the patient face to face. The sEMG signal of the physiotherapist's upper arm are transmitted to the system through the surface electromyography (sEMG) sensor in the MYO armband, so that it can realize the motion reconstruction of the driven end, thereby helping patients with heterolateral motion rehabilitation. To confirm the effectiveness of the system, the master-end elbow joint motion angle estimated by the sEMG signal are compared with the actually grasped hetero-slave-end motion angle obtained from the IMU by us. At the moment, the control accuracy of the mechanical system and the recognition accuracy of the prediction period are analyzed by us. The experiment proves the feasibility of this master-slave heterolateral elbow rehabilitation robot system.**

Index Terms - MYO Armband, Heterolateral Elbow Joint Rehabilitation, Master-Slave Robot Estimated Accuracy.

I. Introduction

According to the 2017 *Global Burden of Disease, Injury and Risk Factor Study*, stroke is the second leading cause of death and the third leading cause of disability in the world [1]. As the largest country in the world for stroke, China currently has as many as 15 million living patients with the disease, with an average of 1 new stroke every 12 seconds. Damage to the central nervous system caused by stroke can lead to impaired motor control of the upper and lower extremities. Due to the limited rehabilitation medical conditions, the hemiplegia rate of stroke in my country is as high as 80%-90%, and the disability rate is 2.5 times that of the United States [2]. This has caused great trouble to the lives of stroke patients in our country.

Rational rehabilitation training is an effective way to treat stroke patients [3]. After a stroke, patients usually require long-term progressive medical care and exercise rehabilitation, which often requires one-on-one treatment for the patient and a rehabilitation physician [4]. Unfortunately, in low- and middle-income countries where there are relatively more stroke patients, the limited economic budget of patients, inadequate rehabilitation care, and the shortage of traditional occupational physiotherapists makes it difficult for patients to support this personalized physiotherapy recovery. However, with the rapid development of robotics technology in the past few decades and the widespread application of rehabilitation concepts in the field of robotics, there has been a positive promotion of health care measures around the world. It can be said that the development of rehabilitation robot technology provides a broader application group for sports rehabilitation [5][6].

To help stroke patients with rehabilitation training, researchers have developed rehabilitation robotic systems such as Soft Exosuit [7] and ANYexo [8]. These assistive devices can provide therapists and patients with programmable levels of assistance. However, due to the impact of the new crown epidemic in recent years, contact rehabilitation methods often bring high safety hazards, and it is difficult to meet the rehabilitation needs of the increasing number of stroke patients. In order to relieve the pressure of these patients, the researchers first chose to study the telerehabilitation robot system, hoping that physical therapists could help stroke patients with sports rehabilitation training through remote online guidance. Mario Cortez et al. designed a novel mechatronics master-slave hand tele-rehabilitation device to help rehabilitation specialists remotely observe the data of patients' hand rehabilitation movements and assist in treatment [9]. Ismail Ben Abdallah et al. designed a wrist telerehabilitation system [10], which allows the physiotherapist to transmit force signals to the patient by applying force to the manipulator. Yi Liu et al. designed a home based tele-rehabilitation system with enhanced therapist-patient remote interaction to achieve rehabilitation exercise in the home environment [11]. However, in the actual application process, telerehabilitation usually requires patients to purchase slave-side rehabilitation robots, signal acquisition equipment and supporting computers, which is a big burden for most families. In addition, researchers have also tried traditional bilateral rehabilitation robotic systems [12], such as Cara G. Welker et al. To develop a system for amputees that

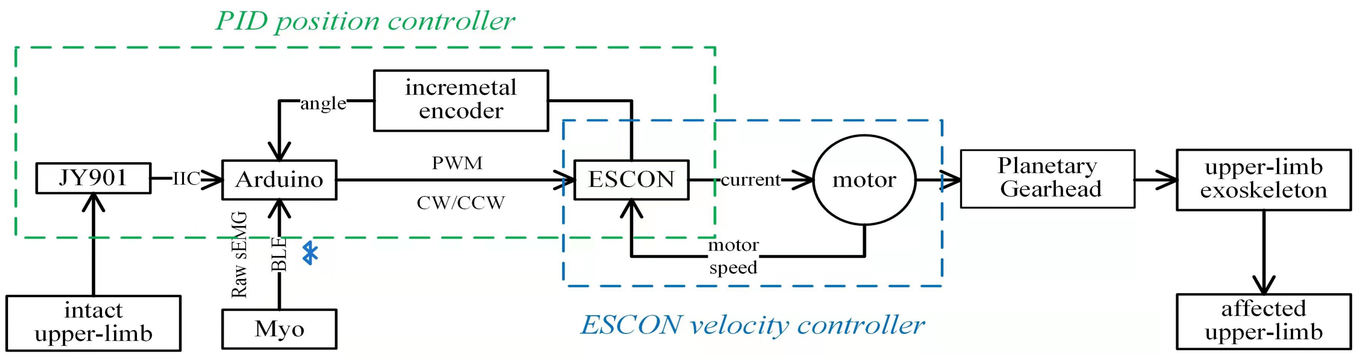

Fig. 1 System architecture. The sEMG data are collected by the MYO armband, and the rotation angle of the forearm is given by the JY901 sensor placed on the upper-limb. They are processed by the Arduino transmitted to the ECSON with PID angle control via the encoder.

non-invasively restores missing control and sensory information in ankle-foot prostheses [13]. The device allows the wrist exoskeleton to receive motion feedback signals from the prosthetic limb to improve patients' overall control and help them learn rehabilitation movements. Such as Y Liu et al. A variable stiffness bilateral exoskeleton device for elbow rehabilitation was developed [14]. The device can autonomously adjust joint stiffness based on the strength of the patients' sEMG signal, providing patients with good exercise assistance. However, such bilateral rehabilitation robots often lack the constant guidance of physical therapists, and are usually only suitable for patients with good rehabilitation training experience. For most patients, rehabilitation therapy is a relatively subjective treatment method that relies on rehabilitation physicians. The lack of intuitive help from rehabilitation physicians often leads to patients' lack of trust in the entire treatment process, thus affecting the rehabilitation effect. In order to solve these two problems, we tried to combine the concepts of bilateral rehabilitation and master-slave rehabilitation, and combined with the problem that doctors are prone to muscle fatigue during long-term unilateral exercise, and proposed a master-slave heterolateral rehabilitation system.

In this paper, we propose a master-slave heterolateral elbow rehabilitation robot based on the MYO arm ring, which can achieve non-contact treatment at a safe distance (above 1.5m) through MYO's Bluetooth transmission device, and can achieve The lateral control method prevents the muscle fatigue phenomenon caused by the long-term single upper limb movement of the rehabilitation therapist, thereby improving the working time and rehabilitation efficiency of the rehabilitation therapist. At the same time, patients can avoid safety problems during the epidemic while ensuring the efficiency of face-to-face consultations through its rehabilitation exercises under the control of physical therapists outside the safety line. The physiotherapist wears a MYO armband with an 8-channel sEMG sensor on the upper arm and binds the IMU sensor to the wrist. The movement direction of the elbow can be measured and calculated by the IMU sensor, and then the movement direction of the wrist can be calculated. The system can reconstruct the movements of the therapist's upper arm and use the exoskeleton robot to drive the patient's ipsilateral arm to perform the same movements to complete personalized rehabilitation training.

The rest of the paper is organized as follows. The experimental protocol and processing methods are illustrated in Section II. In Section III, the results and discussion are reported. Finally, the conclusion is presented in Section IV.

II. STRUCTURE AND SYSTEM

The hardware device of rehabilitation which composed of three parts (a mechanical structure, a sensor system, and a control system) proposed and used a bilateral rehabilitation concept. The control system includes position control based on PID and speed control based on ESCON, that give the device a precise control of position and speed. These three parts work together to enable the upper limb rehabilitation robot elbow rehabilitation training. Fig. 1 is a schematic diagram which describing the system architecture and communication.

A. Upper Limb Rehabilitation Exoskeleton Robot

In our research, we imitate the existing upper limb exoskeleton rehabilitation robot for modeling, and make simple improvements to its transmission structure, as shown in Fig. 2. Keep the gear transmission between the motor and the mechanical structure unchanged, and improve it with a sleeve and a retaining ring to reduce its transmission loss. The whole frame is changed from aluminum alloy to UV resin design, assembled with socket head screws. This rehabilitation structure greatly reduces the wearing burden on the affected side of the patient while providing basic support. The entire exoskeleton is less than 1kg, which is lighter and has less transmission loss than previously designed upper limb rehabilitation robots [15]. Because of that, the patient will not feel fatigue easily after wearing it. It can complete elbow flexion/extension to meet the basic rehabilitation needs.

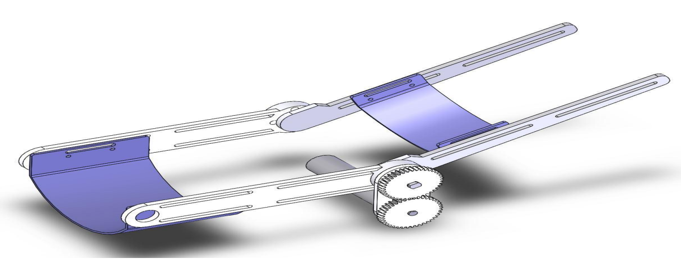
Fig. 2 The upper limb rehabilitation robot model.

Fig. 2 is the structure of elbow rehabilitation robot. According to past experiments, human`s normal elbow motion range are 0~135°, but since the rigidity of UV resin is lower than that of the aluminum alloy material, the maximum range of motion of the elbow joint of the mechanical structure of the elbow joint is set to 5~130°. The limited angle of mechanical structure aim to make the device suitable for the rehabilitation of patients with different clothes, and also avoids the robot to go beyond the physiological motion range.

The entire skeleton is attached to the subject's upper arm and forearm by square grooves and Velcro strips. The tightness of the square groove can be adjusted to suit different patients and avoid performance degradation due to mismatch between patients and rehabilitation equipment.

At the initial moment, the subject wore the upper limb rehabilitation robot on the affected side (in this experiment, the left arm with relatively weak muscle strength was positioned on the affected side), and ensured that the arm was completely detached.

B. *MYO Armband*

The MYO armband which designed by Canadian firm Thalmic Labs is equipped with 8 sEMG sensors. The sampling frequency of the sEMG signal is able to achieve 200 Hz. The data acquired from MYO armband could be transmitted to the microprocessor or computer via its Bluetooth module [16].

The MYO armband is very parctical for our experiments compared to other tranditional sEMG data acquisition. Thanks to its expandable elasticity, it can be put on and taken off easily and can be adjusted to any forearm size.

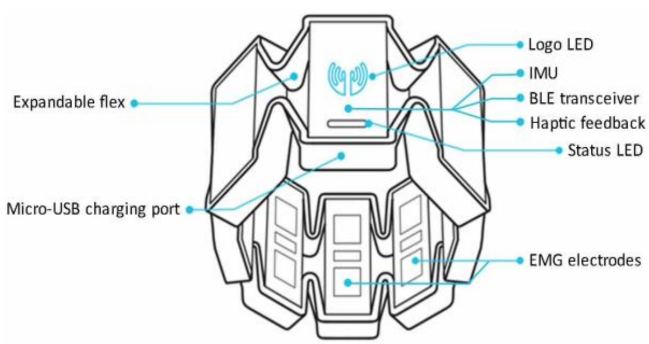

Fig. 3 MYO gesture control armband.

Fig. 3 shows the each part of structure module of the MYO. The Bluetooth module of that can receive the sEMG data from the MYO armband and transfer it to the Arduino.

III. METHODOLOGY

In this section, we describe the characteristics of the experiment setup, the channel selection of MYO armband, data preprocessing and feature extract.

A. *Experiment setup*

A convenience sample of 24 consecutive healthy subjects recruited from our laboratory are rolled in the study, 20 sets of samples are used for modeling, and 4 groups of samples are used for error detection, as shown in TABLE I. In the experiment, members of the modeling group used a blind selection method to pick out the master and the slave, and ensure that all members have become the master or the slave at least once.

TABLE I
SUBJECT POPULATION INFORMATION

	Gender	Number	Age
Modeling object	Man	12	22-29
	Woman	7	22-25
Test object	Man	3	24,29
	Woman	2	24,25

The MYO armband is worn on the right upper arm of the subject-master as the main control arm, and the sEMG signals of each channel are acquired. At the same time, the elbow joint rehabilitation robot was fixed on the subject-slave's left arm to perform auxiliary movements, and the JY901 gyroscope was fixed on the subject-slave's wrist to measure the positive rotation angle of the elbow joint.

During the test, subjects were placed 1.5m face-to-face to ensure basic isolation and protective measures in the event of an epidemic. The subject-master used a relatively stable master side operating arm, and performed 60 seconds of front elbow rehabilitation flexion and extension training according to the body position. At the same time, the subject-slave maintained a de-stressed state to follow the movement, as shown in Fig. 4, with a 5-minute rest interval. Each group of participants performed 10 groups, and finally 60 groups were randomly selected for data analysis. During this period, the slave-side rehabilitation robot don`t have any faults such as response termination, and the motion trajectory did not exceed the normal range of motion of the human elbow joint.

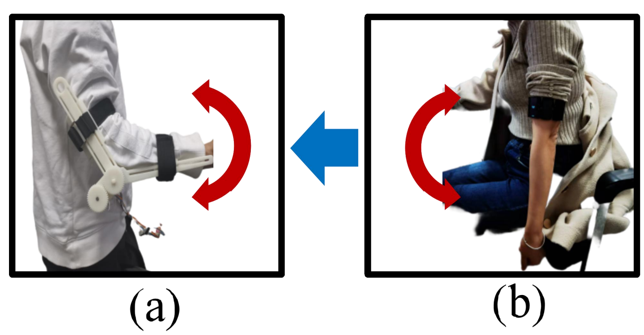

Fig. 4 Diagram of upper limb movement. (a) Slave end's movement diagram. (b) Master end's movement diagram.

B. *Estimation of elbow angle by sEMG signal*

sEMG is a kind of biological signal which can be recorded and evaluate human skeletal muscle tension and control related motion. And it can be used to reflect the user's action intention. Moreover, sEMG signals also can be used to detect the intention of movement, predict joint torques and angles, synthesize the movement of the robotic arm, and guide the rehabilitation of the paralyzed arm.

1) sEMG channel selection: In the forward flexion of the elbow, the biceps, brachial, and triceps are involved in upper limb movement. In order to ensure that the collected sEMG

signals can fully reflect the activities of the upper arm muscles during elbow flexion as far as possible under the premise of reducing the computation of neural network, we select the corresponding channel-1 (brachial), channel-4 (the biceps), channel-7 (triceps). The corresponding positions of muscle and sEMG acquisition channels are shown in the Fig. 5.

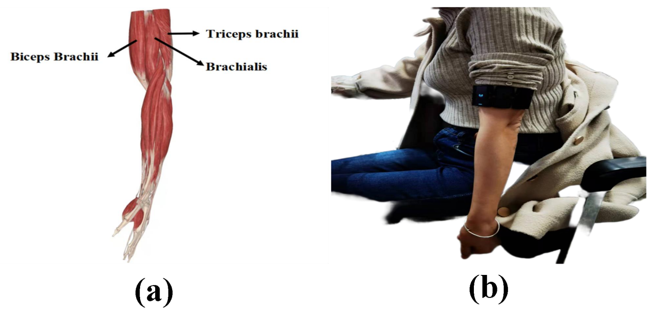

Fig. 5 (a) Muscle model of upper limb; (b) MYO wearing schematic

2) Active segment extraction: Because of the starting time of sEMG signal acquisition not synchronous with elbow Angle information acquisition, we choose to intercept the valid fragments of synchronization and determine whether its energy exceeds the threshold to ensure the corresponding between the sEMG data and the angel data. The formula is described as follows:

$$Q = \int_{t_i}^{t_i+\Delta t} semg(t)^2 \, dt \, . \tag{1}$$

As shown in (1): Q is the energy value of the sEMG/elbow-angle signal in the window, △t is the width of the sliding time window, and *semg*(t) is the collected data of the sEMG/elbow-angle changing with time.

The processed part of the active end signal is shown in the Fig. 6 Among them, Fig. 6(a) is the sEMG signal, and Fig. 6(b) is the signal corresponding to the angle of motion of the elbow joint, and the ratio of the sampling frequency of the two is 10:1.

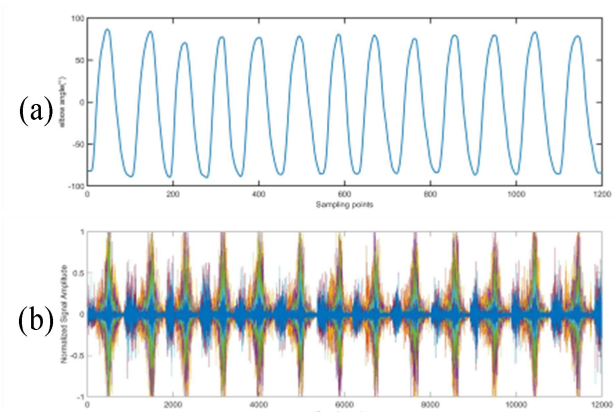

Fig. 6 Sample of angle signal and sEMG signal. (a) Sample of sEMG signal. (b) Sample of angle signal.

3) Signal filtering and normalization: The sEMG signal is complex and weak, and is easily affected by noise during the acquisition process, so need to filter that [17].

In general, the amplitude of sEMG signal is below 5mV, and the main energy is concentrated between 10-150Hz. Since the sEMG signal collected by MYO has been clear of 50Hz power frequency interference, and the sampling frequency of the MYO sensor is 200Hz. So in preprocessing, the signal selected by the master side pass through a the second-order Butterworth high-pass filter (with pass-band cut-off parameter of 20 and s top-band cut-off of 10). After signal filtered, it will be normalized.

$$y = (y_{\max} - y_{\min}) \times \frac{x - x_{\min}}{x_{\max} - x_{\min}} + y_{\min} \, . \tag{2}$$

As shown in the (2), the maximum value y_{max} and the minimum value y_{min} of y are set as +1 and -1 respectively, where x represents the value of the signal sample, and x_{max} and x_{min} represent the maximum and minimum amplitudes of the signal.

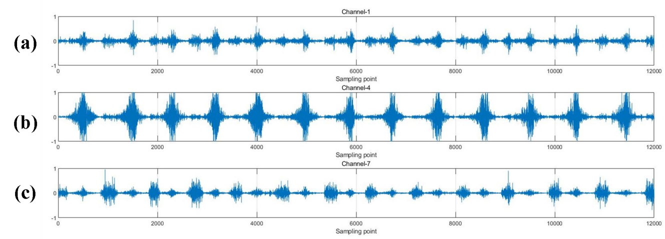

Fig. 7 The processed sEMG signal of the three muscles. (a) Channel-1 preprocessed sEMG signal. (b) Channel-4 preprocessed sEMG signal. (c) Channel-7 preprocessed sEMG signal.

4) Feature extraction: Feature extraction is an important step in applying sEMG signal to neural network training. Signal feature extraction methods usually include time domain method, frequency domain method, time frequency domain method and high order spectral analysis method.

The time domain characteristics of sEMG signal can reflect its assignment characteristics, and its frequency domain characteristics can reflect the individual differences between acquisition objects and fatigue degree. In order to obtain the relationship between the sEMG signal value assigned and the motion amplitude of the elbow joint, and to further improve the accuracy of the model, 6 temporal characteristics are selected to be extracted: the integrated absolute value(f_{IAV}), the logarithmic detection(f_{LogD}), the maximum average amplitude(f_{MAv}), the maximum amplitude(f_{MAX}), root mean square(f_{RMS}), variance (f_{VAR}), wave length(f_{WL}).

$$f_{\mathrm{IAV}} = \frac{\sum_{1}^{N-1} |x_i|}{N^2} \, . \tag{3}$$

$$f_{LogD} = e^{\frac{\sum_{1}^{N-1} \lg |x_i|}{N}} \, . \tag{4}$$

$$f_{MAV} = \frac{\max(|x_i|)}{N}, i < N \, . \tag{5}$$

$$f_{MAX} = \max(|x_i|), i < N \, . \tag{6}$$

$$f_{RMS} = \sqrt{\frac{\sum_{1}^{N-1} x_i^2}{N}} . \quad (7)$$

$$f_{VAR} = \frac{\sum_{1}^{N-1} \left(\frac{\sum_{1}^{N-1} x_i}{N} - x_i\right)^2}{N} . \quad (8)$$

$$f_{WL} = \frac{\sum_{2}^{N-1} |x_i - x_{i-1}|}{N} . \quad (9)$$

Where N is the number of samples in a separate window, x_i represents the i[th] sample within an analysis window.

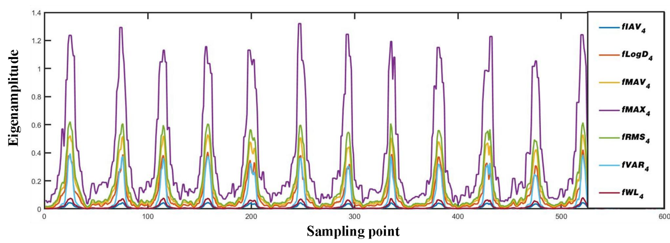

Fig. 8 channel-4 characteristic curve.

5) Back propagation neural network (BPNN) training and prediction: BPNN is a kind of multilayer feed-forward neural network, the main characteristics of it are that: the signal is forward propagation, and the error is backward propagation.

In order to verify the feasibility of "using the subject's upper limb sEMG signal to control the motion angle of the object's heterolateral elbow joint", and to make the entire neural network model maintain real-time performance on the arduino, a BPNN was selected to establish the sEMG signal and elbow angle model. We used a three-layer BP neural network controller. The network structure model is shown in Fig 10. The first layer is the input layer, consisting of three channels with six sEMG characteristic values, and the second layer is the hidden layer with N nodes.

$$n_1 = \sqrt{n+m} + a \quad (10)$$

As shown in the (10), n is the number of input units, m is the number of output neurons and n_1 is the number of neurons in the hidden layer.According to the formula and related experience, the setting n_1=4 in this experiment

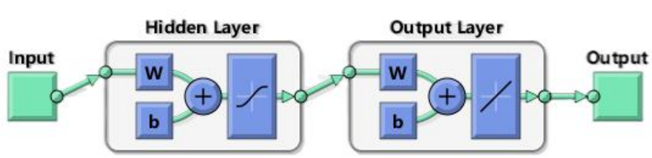

Fig. 9 Three layer BP neural network architecture

C. PID-based master-slave synchronous motion

Proportional-integral-derivative (PID) control, is one of the earliest control strategies developed. Because of its simple structure, good stability, reliable operation and convenient adjustment, it is widely used in industrial control process.

The PID controller is a linear controller that it forms a deviation according to the given value r(t) and the actual output value y(t).

$$e(t) = r(t) - y(t) \quad (11)$$

The proportional (P), integral (I), and differential (D) of the deviation are linearly combined to form a control quantity to control the controlled object. The control law of that is shown in (12).

$$u(t) = K_p e(t) + K_i \int_0^t e(t)dt + K_d \frac{de(t)}{dt} \quad (12)$$

The forward position signal of the elbow joint at the master and slave ends are obtained through JY901, as shown in Fig. 10. In this fomula, K_p is the proportional coefficient, K_i is the integral coefficient; K_d is the differential coefficient. And by virtue of the difference of the collected elbow joint angle signals, PID control is performed on the Arduino control board, so as to realize the real-time follow-up movement from the slave to the master.

IV. EXPERIMENTAL AND RESULT

We compared the elbow joint motion angle signal estimated based on the sEMG signal, the master-end elbow joint motion angle signal obtained by the JY901 sensor, and the slave-end elbow joint motion angle signal obtained by JY901, and get the Angle estimation error between the elbow joint of the master end and the angle following error of slave ends.

TABLE II
MODEL TEST

	The Group of Test	RMSE	Mean
Person22	Test1	1.4769	1.5958
	Test2	1.0525	
	Test3	1.4426	
	Test4	0.8507	
	Test5	3.1563	
Person23	Test1	0.5335	2.1461
	Test2	1.4420	
	Test3	2.2520	
	Test4	1.4206	
	Test5	5.0825	
Person24	Test1	0.7710	3.3377
	Test2	1.8470	
	Test3	3.9252	
	Test4	3.8304	
	Test5	6.3148	

According to Table II, we can find that the sum of estimation error and control error caused by our system for different non-modeling groups is acceptable, and its RMSE is below 5. This control accuracy is similar to the heterolateral control of the same individual [12], which reflects the effectiveness of the control model that uses the master-end individual sEMG signal to control the elbow joint heterolateral movement angle of the slave-end individual.

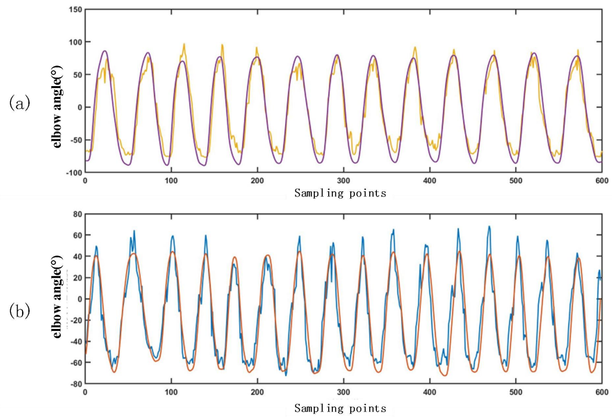

Fig. 10 Comparison of master`s estimated angles and slave`s actual ends;(a)Perison1's estimation, that belongs to the modeler's out-of-model data evaluation; (b)Person24's estimation, that belongs to the non-modeler's data evaluation.

Fig. 10 show that the evaluation effect of existing individuals in the model is better than that of individuals without stored model data. At the same time, the model has some errors in the estimation of sEMG signal at the peak. Since the elbow joint rehabilitation robot we designed uses UV material as a whole, the overall rigidity is low, so the error at this part of the peak will not damage the safety of the subject's arm.

V. CONCLUSION

In this paper, a novel MYO-based master-slave robotic system for heterolateral elbow rehabilitation is proposed. Among them, the frame structure of the slave robot is designed and improved by SolidWorks software, and printed and spliced with UV resin. This paper introduces the master-slave control system framework of the robot. Under the condition of ensuring the accuracy of the master-slave PID control and speed control, the BPNN neural network model is used to determine the slave-side heterolateral elbow joint movement angle through the master-side upper limb sEMG signal. And then, the model is made in its predictions and that is analyzed in its prediction accuracy. The experimental results show that it is effective to use the master-slave system to predict and control the motion angle of the patient's heterolateral elbow joint through the sEMG signal of physiotherapist's upper limb.

In the future, we will improve the rehabilitation range, freedom of movement and portability of the exoskeleton robot platform on which the system is based, thereby improving the application performance of the slave device. At the same time, we will optimize the performance of master-slave control and the motion angle estimation model to solve the problems of control delay and angle deviation during robot motion. In addition, we will combine the driving force information with the robot remote control system through the HD2 device to realize the driving force transmission between the doctor and the patient, thereby improving the personalized performance of the system.

REFERENCES

[1] T. Vos, A. A. Abajobir, K. H. Abate, C. Abbafati, K. M. Abbas, F. Abd-Allah, et al, "Global, regional, and national incidence, prevalence, and years lived with disability for 328 diseases and injuries for 195 countries, 1990 — 2016: a systematic analysis for the Global Burden of Disease Study 2016," *The Lancet*, vol. 390, no. 10100, pp. 1211 — 1259, November 2018.

[2] GBD 2019 Stroke Collaborators, "Global, regional, and national burden of stroke and its risk factors, 1990-2019: a systematic analysis for the Global Burden of Disease Study 2019," *Lancet Neurology*, vol. 20, no 10, pp 795-820, September 2021, doi:10.1016/S1474-4422(21)00252-0.

[3] M. Klaic, J. Fong, V. Crocher, K. Davies, K. Brock, E. Sutton, D. Oetomo, Y. Tan, M. Galea, "Application of the extended technology acceptance model to explore clinician likelihood to use robotics in rehabilitation," *Disability and rehabilitation: Assistive Technology*, pp. 1-8, April 2022, DOI: 10.1080/17483107.2022.2060356, PMID: 35400278.

[4] S. M. Hatem, S. Geoffroy, D. F. Margau et al, "Rehabilitation of Motor Function after Stroke: A Multiple Systematic Review Focused on Techniques to Stimulate Upper Extremity Recovery," *Frontiers in Human Neuroscience*, vol. 10, 2016.

[5] F. Ferreira, M. Chaves, V. Oliverira, J. Martins, C. Vimieiro, A. Petten, "Effect of Robot-Assisted Therapy on Participation of People with Limited Upper Limb Functioning: A Systematic Review with GRADE Recommendations," *Occupational therapy international*, vol. 2021 6649549, July 2021, doi:10.1155/2021/6649549.

[6] J. M. Veerbeek, A. C. Langbroek-Amersfoort, E. E. van Wegen, C. G M Meskers, G. Kwakkel, "Meskers CG, Kwakkel G. Effects of robot-assisted therapy for the upper limb after stroke: a systematic review and meta-analysis," *Neurorehabil Neural Repair*, vol. 31, no. 2, pp. 107 — 121, 2017.

[7] Y. Ding, M. Kim, S. Kuindersma, and C. J. Walsh, "Human-in-the-loop optimization of hip assistance with a soft exosuit during walking," *Science Robotics*, vol. 3, no. 15, pp. eaar5438, February 2018.

[8] Y. Zimmermann, A. Forino, R. Riener and M. Hutter, "ANYexo: A Versatile and Dynamic Upper-Limb Rehabilitation Robot," *IEEE Robotics and Automation Letters*, vol. 4, no. 4, pp. 3649-3656, October 2019.

[9] Z. Liu, J. Wu, L. Wang, B. Zhang, "Control Parameters Design Based on Dynamic Characteristics of a Hybrid Robot With Parallelogram Structures," *IEEE/ASME Transactions on Mechatronics*, vol. 26, no. 2, pp. 1140-1150, 2021.

[10]Y. Bouteraa, I. B. Abdallah, A. Ibrahim, T. A. Ahanger, "Fuzzy logic-based connected robot for home rehabilitation," *Journal of Intelligent & Fuzzy Systems*, vol. 40, no. 3, pp. 4835, 2021.

[11]Y. Liu, S. Guo, Z. Yang, H. Hirata, T. Tamiya, "A Home-based Tele-rehabilitation System with Enhanced Therapist-patient Remote Interaction: A Feasibility Study," *IEEE Journal of Biomedical and Health Informatics*, JBHI-01812-2021.R2, in Press, 2022.

[12]Z. Yang, S. Guo, Y Liu, H. Hirata, T. Tamiya, "An intention-based online bilateral training system for upper limb motor rehabilitation," *Microsyst Technol*, vol. 27, pp. 211—222. 2021. doi:10.1007/s00542-020-04939-x.

[13]C. G. Welker, V. L. Chiu, A. S. Voloshina, S. H. Collins and A. M. Okamura, "Teleoperation of an Ankle-Foot Prosthesis With a Wrist Exoskeleton," *IEEE Transactions on Biomedical Engineering*, vol. 68, no. 5, pp. 1714-1725, May 2021.

[14]Y. Liu, S. Guo, H. Hirata, H. Ishihara, and T. Tamiya, "Development of a powered variable-stiffness exoskeleton device for elbow rehabilitation," *Biomed Microdevices*, vol. 20, 2018, doi: 10.1007/s10544-018-0312-6.

[15]B. Gao, H. Ma, S. Guo, H. Xu, and S. Yang, "Design and evaluation of a 3-degree-of-freedom upper limb rehabilitation exoskeleton robot," *International Conference on Mechatronics and Automation*, pp. 938-942, Aug. 2017.

[16]Thalmic Labs. 2013. Available: https://www.myo.com/. (Accessed 1November 2017).

[17]D. Bu, S. Guo, L. He, "sEMG-Based Motion Recognition of Upper Limb Rehabilitation Using the Improved Yolo-v4 Algorithm," *Life (Basel, Switzerland)*, vol. 12, no. 1, pp. 64, Jan. 2022, doi:10.3390/life12010064.